Supporting Information for

Nitrogen-Rich Metal-Free Salts: a New Look at 5-(Trinitromethyl)tetrazolate Anion as an Energetic Moiety

Daniil A. Chaplygin,[a] Alexander A. Larin,[a] Nikita V. Muravyev,[b] Dmitry B. Meerov,[b] Ekaterina K. Kosareva,[b] Vitaly G. Kiselev,[b,c,d] Alla N. Pivkina,[b] Ivan V. Ananyev,[e] and Leonid L. Fershtat*[a]

[a] Zelinsky Institute of Organic Chemistry, Russian Academy of Sciences, 47 Leninsky Ave., 119991 Moscow, Russia. E-mail: fershtat@bk.ru

[b] Semenov Federal Research Center for Chemical Physics, Russian Academy of Sciences, 4 Kosygina Str., 119991 Moscow, Russia

[c] Novosibirsk State University, 1 Pirogova Str., 630090 Novosibirsk, Russia

[d] Institute of Chemical Kinetics and Combustion, Siberian Branch of Russian Academy of Sciences, 3 Institutskaya Str., 630090 Novosibirsk, Russia

[e] Nesmeyanov Institute of Organoelement Compounds, Russian Academy of Sciences, 28 Vavilova Str., 119991 Moscow, Russia

Table of Contents

S1. Crystallographic data

Crystal structures of salts **4** and **5** were previously reported.[1] For **6**, the intensities of 45142 reflections were measured with a Bruker APEX 2 Duo CCD diffractometer [λ(MoKα) = 0.71072Å, ω-scans, 2θ<61°]. The crystals were found to be twins (the CELL_NOW program) with two domains rotated against each other by ~179° (the ratio of domain populations is approximately 4:1). The postprocessing indicates that **6** ($C_5H_7N_{15}O_6$, M = 373.26) crystallizes in monoclinic system, space group $P2_1/c$. At 120K: a = 10.9617(5) Å, b = 12.9060(6) Å, c= 10.4101(5) Å, β = 112.555(2)°, V = 1360.1(1) Å^3, Z = 4 (Z' = 1), d_{calc} = 1.823 g·cm^{-3}, μ(MoKα) = 0.90 cm^{-1}, F(000) = 760. The intensity data were integrated by the SAINT program[2] and were corrected for absorption and decay using the TWINABS routine. The 3974 independent reflections [R_{int} = 0.0479] were used in further refinement. The structure was solved by direct method and refined by using SHELXS[3] and the full-matrix least-squares technique against F^2 in the anisotropic-isotropic approximation using SHELXL-2018.[4] The H(C) atom positions were calculated on the basis of geometric criteria and refined in the isotropic approximation within the riding model. The final refinement was performed taking into account both domains with the HKLF5 instruction. For **6**, the refinement converged to wR2 = 0.1229 and GOF = 1.010 for all independent reflections (R_1 = 0.0504 was calculated against F for 2475 observed reflections with I>2σ(I))**.** CCDC number 2094116 contains all supporting crystallography information and other refinement details.

Crystal density decomposition calculations. The quantum chemistry calculations were performed using the Gaussian 09 program.[5] The geometry of the isolated anion of **6** was optimized at PBE0/def2-TZVP level of theory.[6] In the case of **3 – 6**, the densities of the crystals were decomposed in the framework of the $\mathbf{\Delta}_{OED}$ approach using the HF/3-21G wave functions and electron densities of the isolated ions and crystal fragments. The X-H bond lengths were normalized on the ideal values and the crystal geometry was hold during the calculations. The crystal fragments were generated as charged clusters by computing a symmetry-related shell of the ions surrounding the central molecule with the distance of each interatomic contact being smaller than the sum of corresponding van der Waals radii and 2.0 Å. The volumes of isolated ions were obtained by the integration within the $2\cdot10^{-4}$ a.u. isosurface of electron density. The volumes of the central ions in crystal fragments were calculated by means of the Bader's "Atoms in Molecules" theory.[7] The corresponding integration procedures were performed using the MultiWFN program[8] with the exact refinement of the boundaries of basins.

S2. The Born-Haber Thermodynamic Cycle, Volume-Based Thermodynamics, and Quantum Chemical Calculations of the Thermochemistry of 4 – 9.

The Born-Haber (BH) thermodynamic cycle (Fig. S1) along with the volume-based thermodynamics (VBT) and quantum chemical calculations were employed to estimate the standard (solid-state) enthalpies of formation $\Delta_f H^0_{solid}$ of the energetic salts studied. More specifically, in the framework of the BH cycle, the enthalpies of formation in the crystalline state read as:

$$\Delta_f H^0_{solid} = -\Delta H_{lat} + \left(\Delta_f H^0_{gas}(An^0) + \Delta_f H^0_{gas}(Cat^0)\right) + \Delta H_{PT}, \qquad (1)$$

where $\left(\Delta_f H^0_{gas}(An^0) + \Delta_f H^0_{gas}(Cat^0)\right)$ is a sum of the gas phase enthalpies of formation of the neutral precursors of 5-(trinitromethyl)tetrazolate anion and the cations **4 – 9**, ΔH_{lat} is a lattice enthalpy, and ΔH_{PT} is a proton transfer enthalpy. The lattice enthalpy ΔH_{lat} was estimated using the VBT approach via the empirical formula initially proposed by Jenkins et al.[9]:

$$\Delta H_{lat} = 2\left({\alpha}/{\sqrt[3]{V}} + \beta\right), \qquad (2)$$

where *V* is the molecular volume of the lattice, which is equal to the sum of the volumes of the 5-(trinitromethyl)tetrazolate anion and cations (**4** – **9**) calculated at the B3LYP-D3BJ/def2-TZVPP level, and α and β are empirical parameters. Note that we employed the values proposed particularly for the salts containing nitrogen-rich cations,[10] viz., α = 83.3 (kJ nm)/mol and β = 157.3 kJ mol^{-1}. This parametrization was also shown to perform well for the hydrazinium and ammonium salts of the trinitromethyl cation.[11a] For a neutral compound **3** the sublimation enthalpy was calculated using the reparametrized Westwell-Trouton equation.[11b]

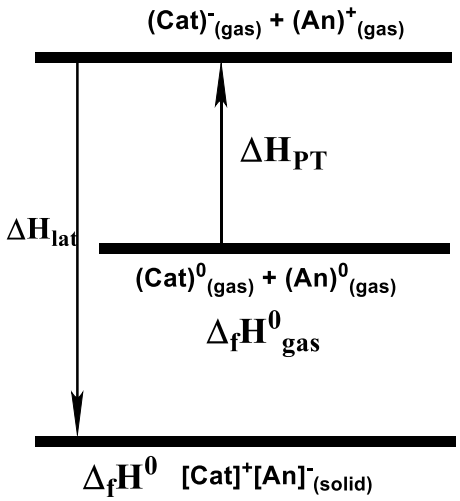

Figure S1. The Born-Haber thermodynamic cycle employed for the estimation of the formation enthalpy of the crystalline salts **4**–**9**.

The breakdown of the enthalpy components is given in Table S1.

Table S1. The Thermochemical Properties of the Salts (Scheme 1 in the Article) and Their Neutral Precursors. All Enthalpy Values are Shown in Figure S1 and are given in kJ mol^{-1}.

#	V, cm^3 mol[a]	ΔH_f^0(gas)[b]	ΔH_{PT}[c]	ΔH_{lat}[d]	$\Delta_f H^0_{solid}$[e]
4	16.1	-44.1	424.1	594.5	188.2
5	42.7	25.0	290.1	578.4	139.6
6	97.2	553.5	281.5	554.4	683.4
7	85.5	572.3	309.1	558.8	725.5
8	57.2	329.0	390.9	571.1	551.7
9	69.6	174.9	334.7	565.4	347.1
TrinitroTz (3)	117.6	402.8			286[f]

[a] The individual ion volumes were taken as those inside the 0.001 a.u. contour of the B3LYP-D3BJ/def2-TZVPP electron density. A Gaussian 09 keyword "volume=tight" (i.e., 100 points per cubic Bohr) was used in the Monte Carlo integration to obtain the desired level of accuracy, a reproducible calculated volume to better than 1%. [b] The gas-phase formation enthalpies of the neutral precursors of 5-(trinitromethyl)tetrazolate anion (**TrinitroTz, 3**) and the cations from **4** – **9** calculated at the W1-F12 level of theory using the atomization energy approach[12]. [c] Calculated at the DLPNO-CCSD(T)/aVQZ level of theory. [d] Calculated using volume-based thermodynamics[9a] and a reparametrized Jenkins formula[10], Eq. (2). [e] Calculated in accordance with Eq (1). [f] The sublimation enthalpy was calculated using the reparametrized Westwell-Trouton equation.[11b]

Electronic structure calculations were performed using the Gaussian 09,[5] Molpro 2010,[13] and ORCA 4.0[14] program packages. The gas phase enthalpies of formation of the neutral precursors of 5-(trinitromethyl)tetrazolate anion and the cations **4** – **9** at p^0 = 1 bar and T = 298.15 K ($\Delta_f H^0_{gas}$) were calculated using the explicitly correlated W1-F12 multi-level procedure[15] and the atomization energy approach described in detail elsewhere.[16] Note that the W1-F12 procedure employed in the present work had been slightly modified in comparison with the originally proposed technique: namely, the B3LYP-D3BJ/def2-TZVPP optimized geometries (the ZPE correction factor of 0.99) were used[17] and the diagonal Born-Oppenheimer corrections were omitted. The W1-F12 procedure employed in the present work for the calculation of $\Delta_f H^0_{gas}$ was benchmarked on a series of energetic high-nitrogen heterocycles and polynitro compounds and exhibited a decent performance close to the average "thermochemical" accuracy (~4 kJ mol^{-1}).[18] The multireference character of the wave functions of the species considered in the present work was estimated using the T1 diagnostic for the CCSD calculation.[19] The modest T1 values obtained in all cases (<0.020) justify the reliability of single reference-based electron correlation procedure

employed in the present study. The heats of formation at 0 K for the elements in the gas phase $\Delta_f H_{gas}^{0K}$(C) = 169.98 kcal mol^{-1}, $\Delta_f H_{gas}^{0K}$(H) = 51.63 kcal mol^{-1}, $\Delta_f H_{gas}^{0K}$(N) = 112.53 kcal mol^{-1}, and $\Delta_f H_{gas}^{0K}$(O) = 58.99 kcal mol^{-1} were taken from the NIST-JANAF tables.[20]

The enthalpies of the proton transfer reactions ΔH_{PT} were calculated using the DLPNO-CCSD(T) methodology (the "NormalPNO" truncation thresholds were set)[21] along with the aug-cc-pVQZ basis set.[22] The RIJK density fitting (DF) approximation[23] was used to accelerate convergence of the SCF components of DLPNO-CCSD(T) energy. The corresponding auxiliary basis sets (aug-cc-pVQZ/JK and aug-cc-pVQZ/C in the ORCA nomenclature)[14] were used in the DF calculations of the SCF and correlation energies.

S3. References

1. Haiges, R.; Christe, K. O. *Inorg. Chem.*, 2013, **52**, 7249-7260.
2. Bruker. APEX-III. Bruker AXS Inc., Madison, Wisconsin, USA, 2018.
3. Sheldrick, G. M. *Acta Crystallogr., Sect. A* **2015**, *71*, 3-8.
4. Sheldrick, G. M. *Acta Crystallogr., Sect. C* **2015**, *71*, 3-8.
5. Frisch, M. J.; Trucks, G. W.; Schlegel, H. B.; Scuseria, G. E.; Robb, M. A.; Cheeseman, J. R.; Scalmani, G.; Barone, V.; Petersson, G. A.; Nakatsuji, H.; Li, X.; Caricato, M.; Marenich, A.; Bloino, J.; Janesko, B. G.; Gomperts, R.; Mennucci, B.; Hratchian, H. P.; Ortiz, J. V.; Izmaylov, A. F.; Sonnenberg, J. L.; Williams-Young, D.; Ding, F.; Lipparini, F.; Egidi, F.; Goings, J.; Peng, B.; Petrone, A.; Henderson, T.; Ranasinghe, D.; Zakrzewski, V. G.; Gao, J.; Rega, N.; Zheng, G.; Liang, W.; Hada, M.; Ehara, M.; Toyota, K.; Fukuda, R.; Hasegawa, J.; Ishida, M.; Nakajima, T.; Honda, Y.; Kitao, O.; Nakai, H.; Vreven, T.; Throssell, K.; Montgomery, Jr., J. A.; Peralta, J. E.; Ogliaro, F.; Bearpark, M.; Heyd, J. J.; Brothers, E.; Kudin, K. N.; Staroverov, V. N.; Keith, T.; Kobayashi, R.; Normand, J.; Raghavachari, K.; Rendell, A.; Burant, J. C.; Iyengar, S. S.; Tomasi, J.; Cossi, M.; Millam, J. M.; Klene, M.; Adamo, C.; Cammi, R.; Ochterski, J. W.; Martin, R. L.; Morokuma, K.; Farkas, O.; Foresman, J. B.; Fox, D. J. Gaussian 09, Revision D.01; Gaussian, Inc.: Wallingford, CT, 2016.
6. (a) Perdew, J.; Ernzerhof, M.; Burke, K. *J. Chem. Phys.* **1996**, *105*, 9982-9985; (b) Adamo, C.; Barone, V. *J. Chem. Phys.* **1999**, *110*, 6158-6170.
7. Bader, R. *Chem. Rev.*, 1991, **91**, 893-928.
8. Lu, T.; Chen, F. *J. Comput. Chem.* **2012**, *33*, 580-592.
9. (a) Jenkins, H. D. B.; Roobottom, H. K.; Passmore, J.; Glasser, L. *Inorg. Chem.* **1999**, *38*, 3609–3620; (b) Jenkins, H. D. B.; Tudela, D.; Glasser, L. *Inorg. Chem.* **2002**, *41*, 2364–2367.
10. Gutowski, K. E.; Rogers, R. D.; Dixon, D. A. *J. Phys. Chem. B* **2007**, *111*, 4788–4800.
11. (a) Kiselev, V. G.; Gritsan, N. P. *J. Phys. Chem. A* **2009**, *113*, 11067–11074; (b) Muravyev, N. V.; Monogarov, K. A.; Melnikov, I. N.; Pivkina, A. N.; Kiselev, V. G. *Phys. Chem. Chem. Phys.* **2021**, *23*, 15522-15542.
12. Curtiss, L. A.; Raghavachari, K.; Redfern, P. C.; Pople, J. A. *J. Chem. Phys.* **1997**, *106*, 1063.
13. Werner, H.-J.; Knowles, P. J.; Knizia, G.; Manby, F. R.; Schutz, M.; Celani, P.; Korona, T.; Lindh, R.; Mitrushenkov, A.; Rauhut, G. et al. MOLPRO, version 2010.1, **2010**.
14. Neese, F. Software update: the ORCA program system, version 4.0. *WIREs Comput. Mol. Sci.* **2018**, *8*, e1327.
15. Karton, A.; Martin, J. M. L. *J. Chem. Phys.* **2012**, *136*, 124114.

16. Curtiss, L. A. *J. Chem. Phys.* **1997**, *106*, 1063.

17. (a) Kesharwani, M. K.; Brauer, B.; Martin, J. M. L. *J. Phys. Chem. A* **2015**, *119*, 1701–1714; (b) Karton, A.; Schreiner, P. R.; Martin, J. M. L. *J. Comput. Chem.* **2016**, *37*, 49-58.

18. (a) Kiselev, V. G.; Goldsmith, C. F. *J. Phys. Chem. A* **2019**, *123*, 4883–4890; (b) Kiselev, V. G.; Goldsmith, C. F. *J. Phys. Chem. A* **2019**, *123*, 9818–9827; (c) Gorn, M. V.; Gritsan, N. P.; Goldsmith, C. F.; Kiselev, V. G. *J. Phys. Chem. A* **2020**, *124*, 7665–7677; (d) Muravyev, N. V.; Monogarov, K. A.; Melnikov, I. N.; Pivkina, A. N.; Kiselev, V. G. *Phys. Chem. Chem. Phys.* **2021**, *23*, 15522-15542.

19. Lee, T. J.; Taylor, P. R. *Int. J. Quantum Chem.* **1989**, *36*, 199-207.

20. Chase, M. W., Jr. NIST-JANAF Thermochemical Tables. *J. Phys. Chem. Ref. Data*, 4th ed.; NIST-JANAF, **1998**; Mono. 9, Suppl. 1.

21. Liakos, D. G.; Sparta, M.; Kesharwani, M. K.; Martin, J. M. L.; Neese, F. *J. Chem. Theory Comput.* **2015**, *11*, 1525–1539.

22. Kendall, R. A.; Dunning, T. H., Jr. *J. Chem. Phys.* **1992**, *96*, 6796.

23. Kossmann, S.; Neese, F. *Chem. Phys. Lett.* **2009**, *481*, 240-243.

S4. DSC Curves and Specific Impulse Values

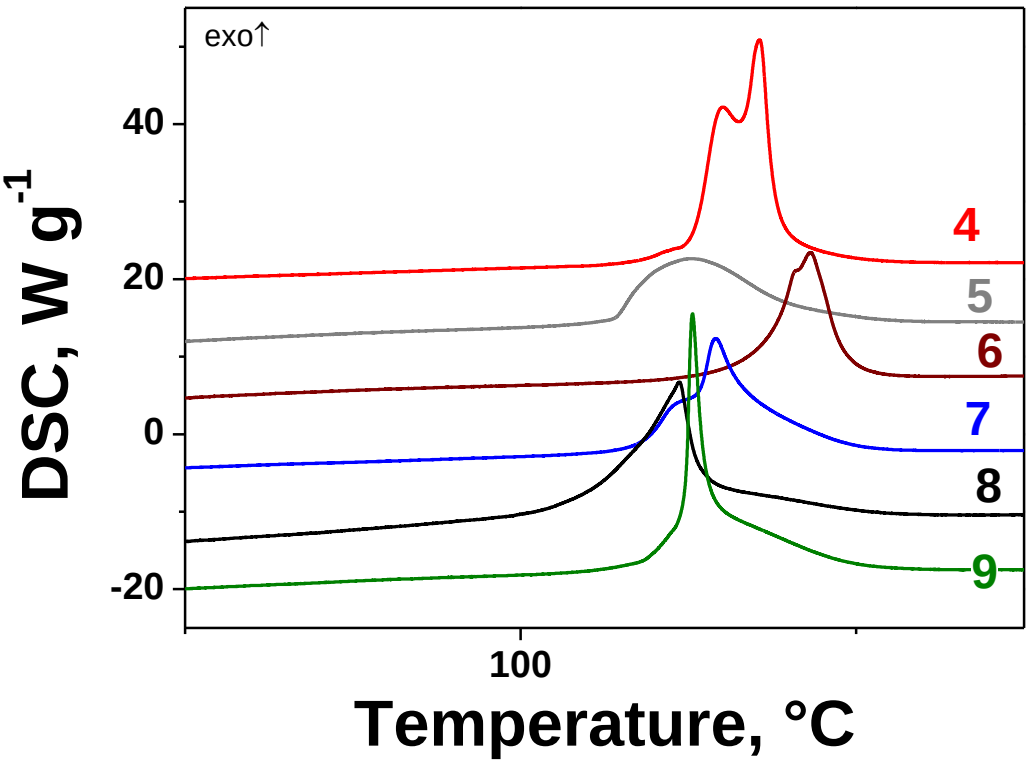

Figure S2. Differential scanning calorimetry for **4** – **9** at linear heating with 5 K min^{-1} rate. Curves are shifted for clarity.

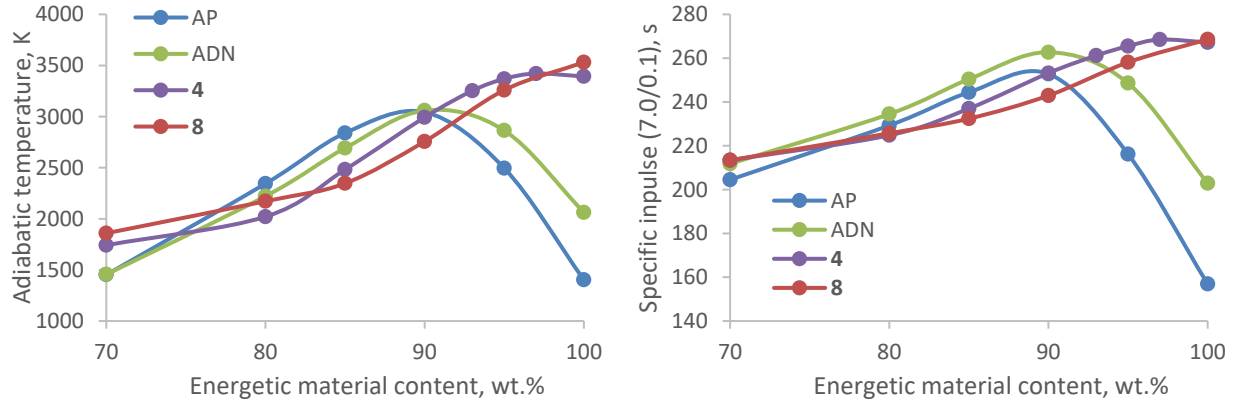

Figure S3. Thermodynamic calculation results for energetic compound (ammonium perchlorate=AP, synthesized salts **4**, **8**, and ammonium dinitramide=ADN) mixture with HTPB binder. Right plot represents the adiabatic temperature, left – the specific impulse for combustion at 7.0 MPa. Calculations were performed in Cproper software [*A. Lefebvre, Cpropep v 1.0, 2000, Thermodynamic Data from B. Mac Bride, NASA Glenn Research Center*].

S5. Copies of NMR Spectra

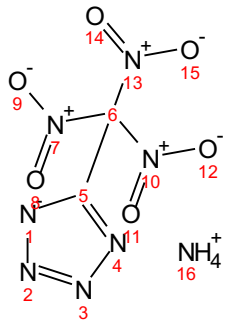

4

^{1}H NMR (300 MHz)

DMSO-d_6

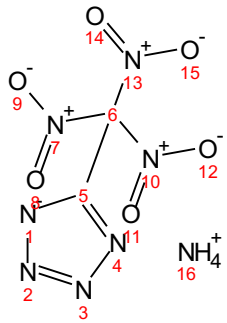

4

^{13}C NMR (75.5 MHz)

DMSO-d_6

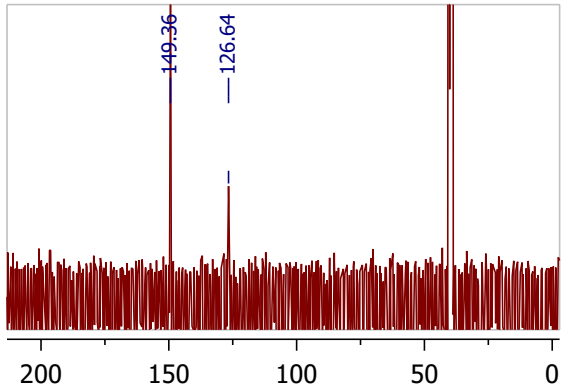

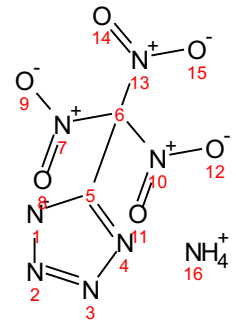

4

^{14}N NMR (21.7 MHz)

DMSO-d_6

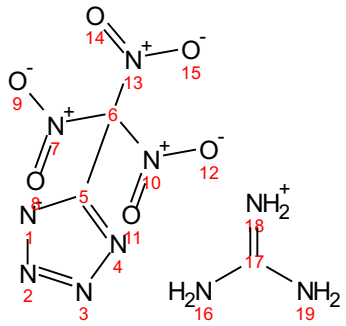

5

^{1}H NMR (300 MHz)

DMSO-d_6

7.18

3.53

2.49

water

DMSO

6.00

15.0 14.5 14.0 13.5 13.0 12.5 12.0 11.5 11.0 10.5 10.0 9.5 9.0 8.5 8.0 7.5 7.0 6.5 6.0 5.5 5.0 4.5 4.0 3.5 3.0 2.5 2.0 1.5 1.0 0.5 0.0

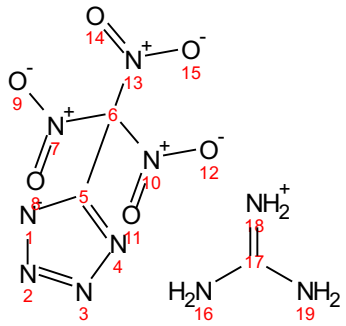

5

^{13}C NMR (75.5 MHz)

DMSO-d_6

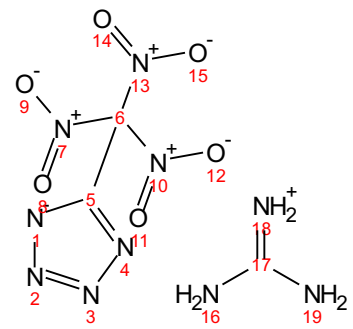

5

^{14}N NMR (21.7 MHz)

DMSO-d_6

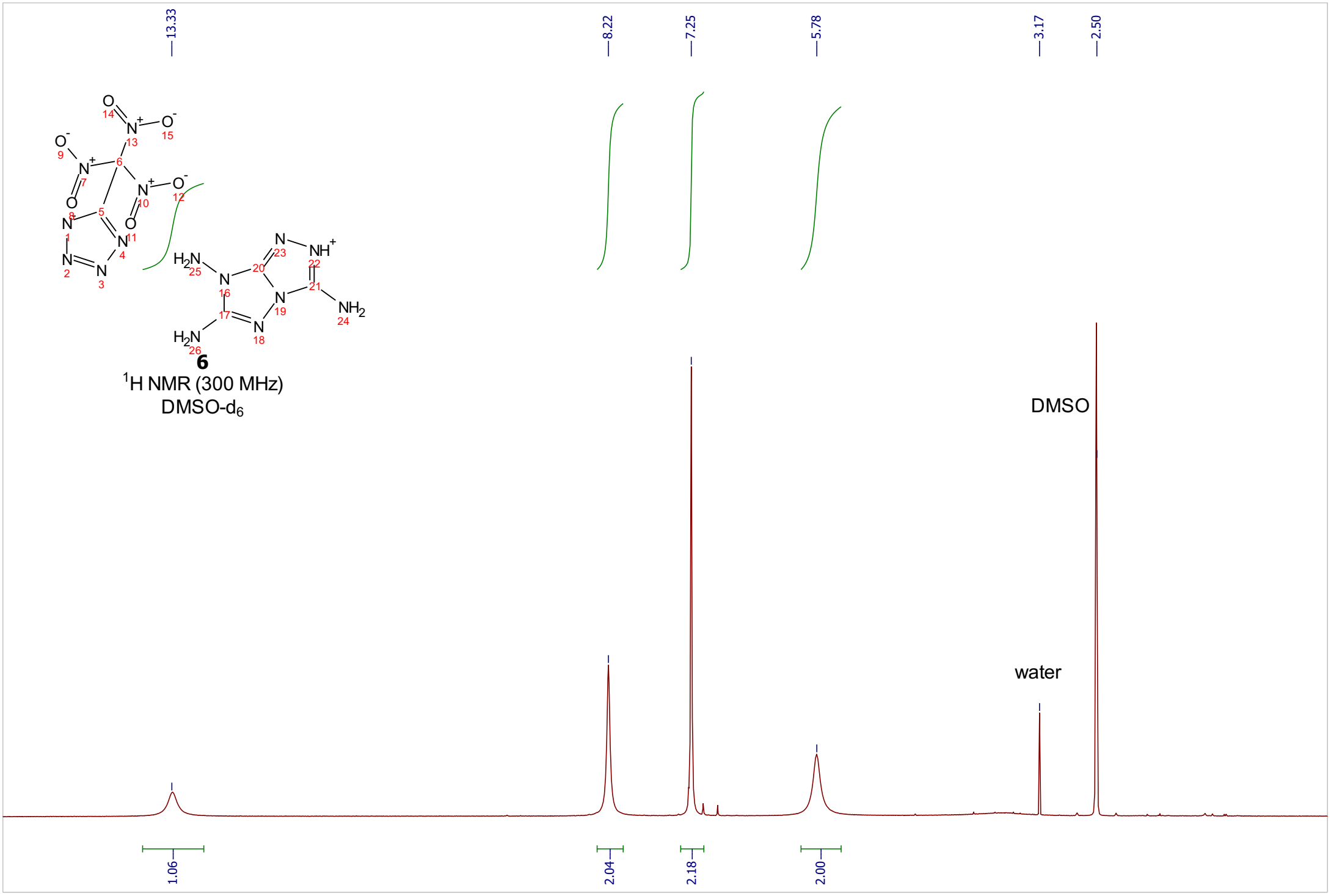
13.33
8.22
7.25
5.78
3.17
2.50
6
1H NMR (300 MHz)
DMSO-d6
DMSO
water
1.06
2.04
2.18
2.00
15.0 14.5 14.0 13.5 13.0 12.5 12.0 11.5 11.0 10.5 10.0 9.5 9.0 8.5 8.0 7.5 7.0 6.5 6.0 5.5 5.0 4.5 4.0 3.5 3.0 2.5 2.0 1.5 1.0 0.5 0.0

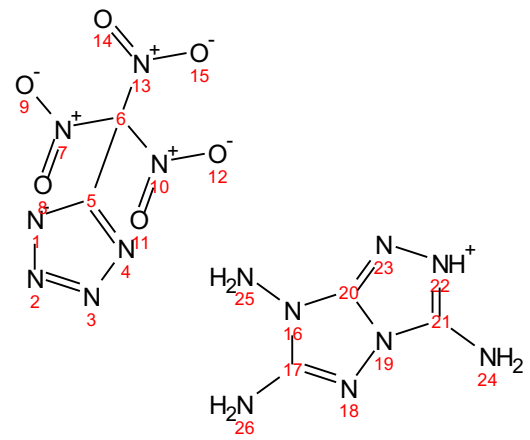

6

^{13}C NMR (75.5 MHz)

DMSO-d_6

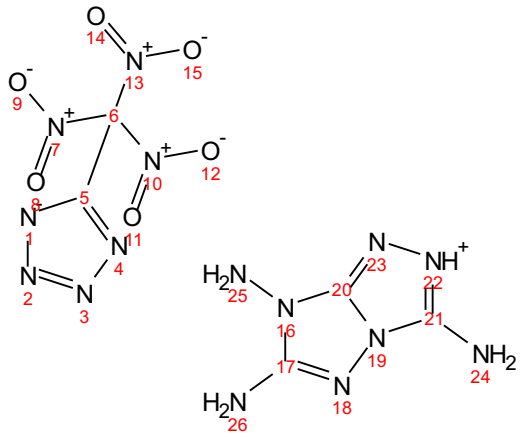

6

^{14}N NMR (21.7 MHz)

DMSO-d_6

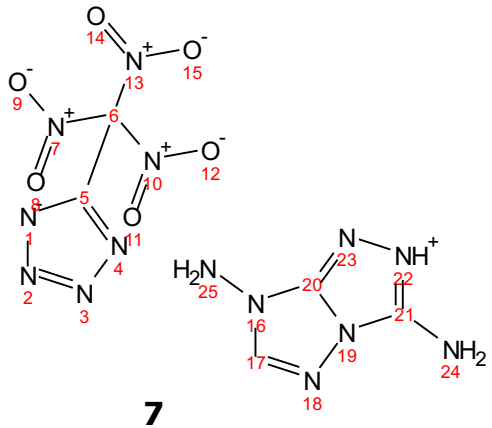

7

^{1}H NMR (300 MHz)

DMSO-d_6

8.85

8.65

6.30

DMSO

1.00

1.91

1.82

15.0 14.5 14.0 13.5 13.0 12.5 12.0 11.5 11.0 10.5 10.0 9.5 9.0 8.5 8.0 7.5 7.0 6.5 6.0 5.5 5.0 4.5 4.0 3.5 3.0 2.5 2.0 1.5 1.0 0.5 0.0

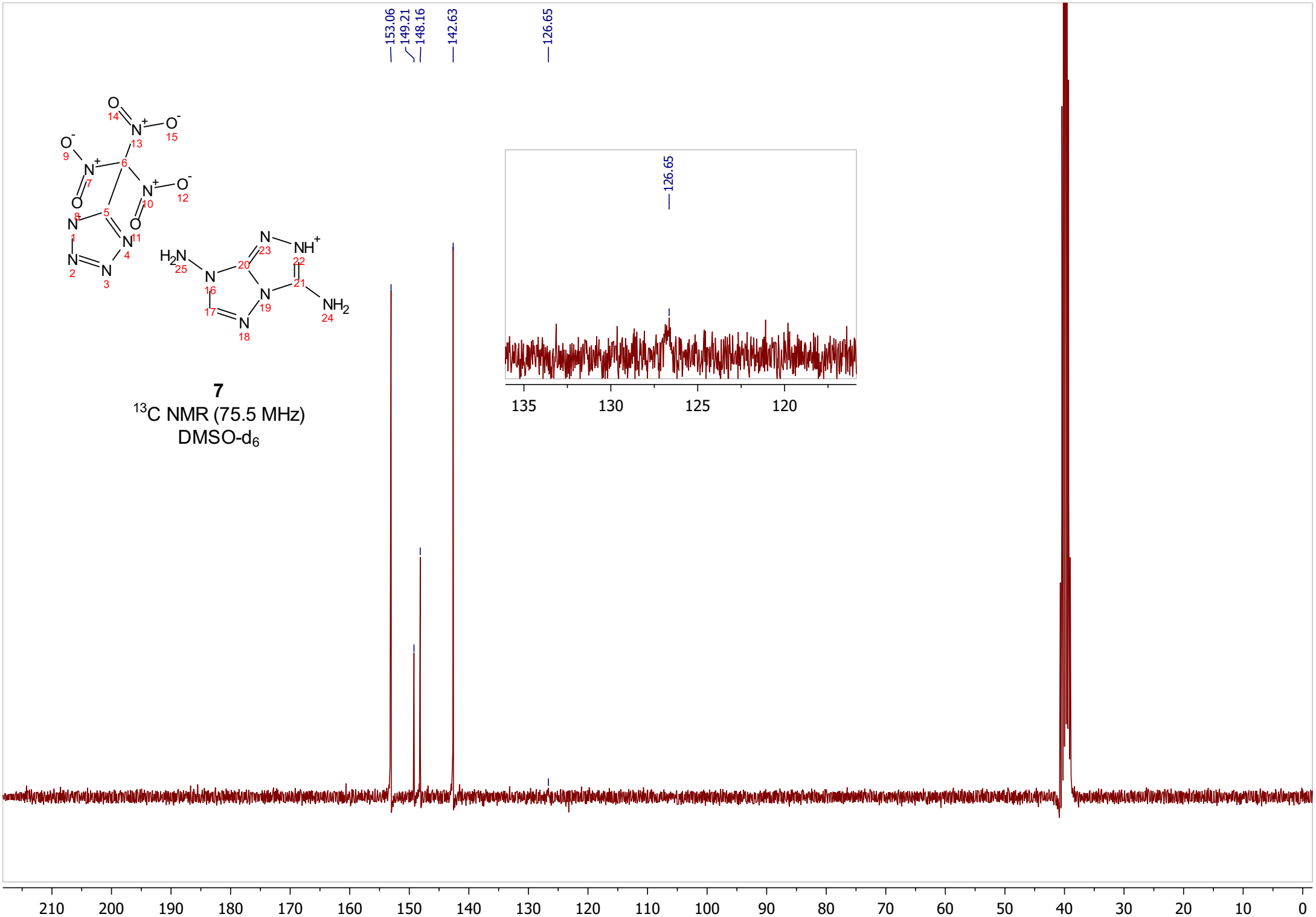

7

^{13}C NMR (75.5 MHz)

DMSO-d_6

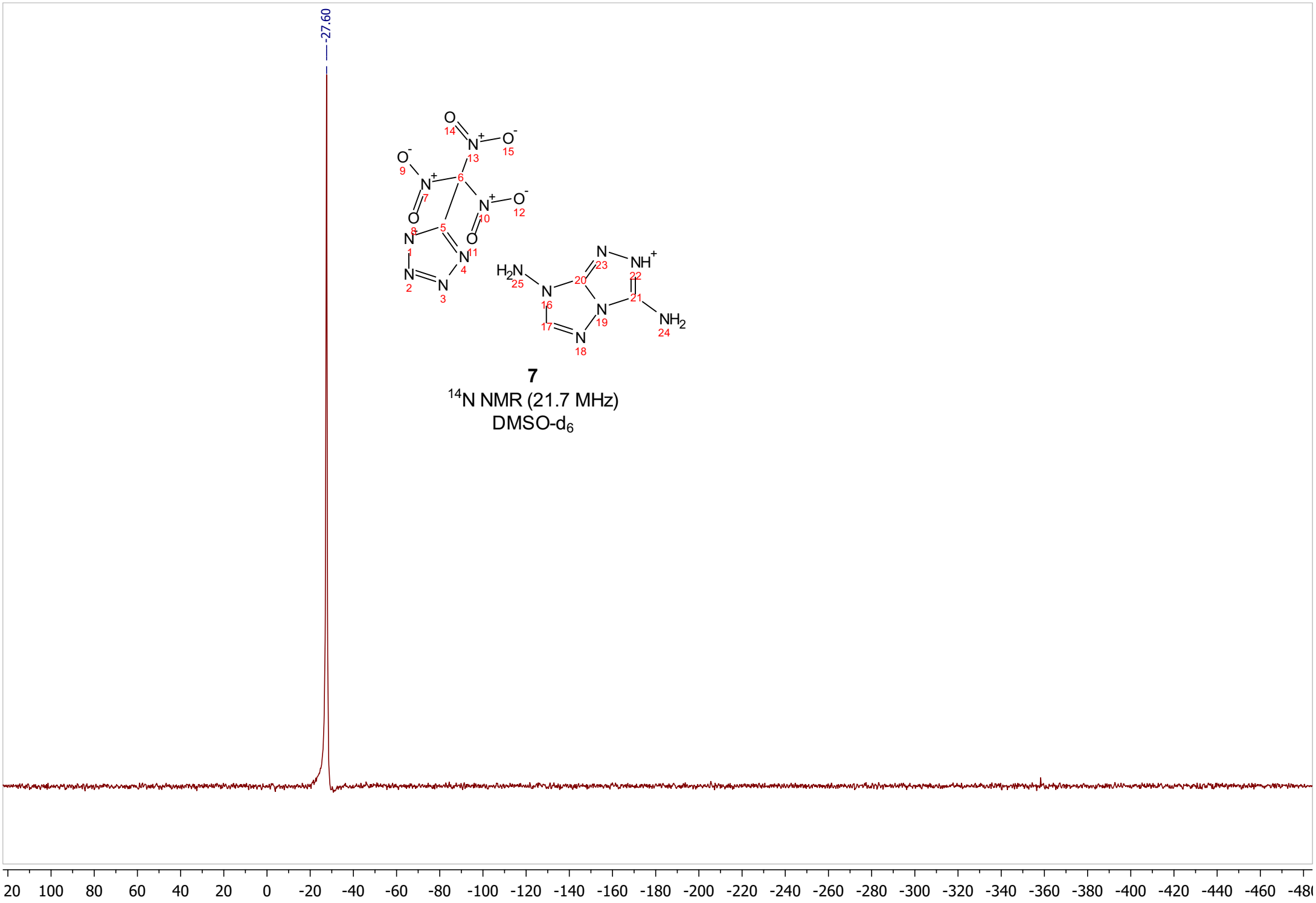

7

^{14}N NMR (21.7 MHz)

DMSO-d_6

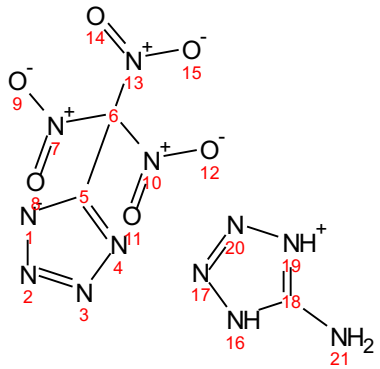

8

^{1}H NMR (300 MHz)

DMSO-d_6

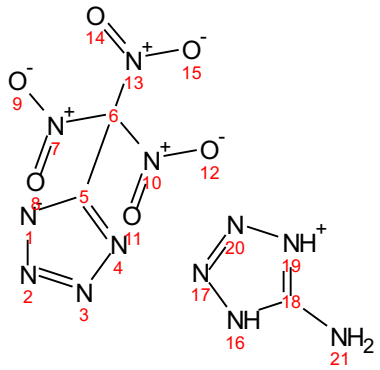

8

^{13}C NMR (75.5 MHz)

DMSO-d_6

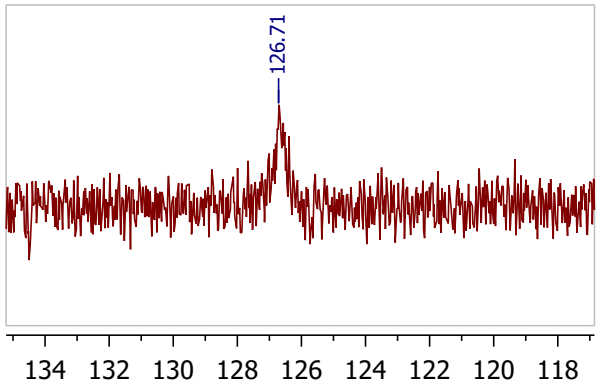

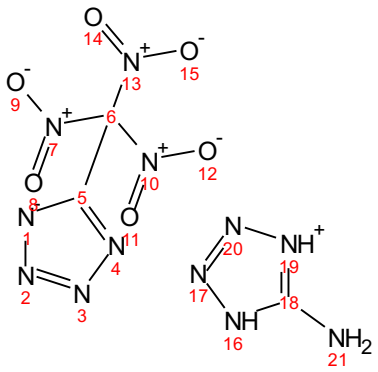

8

^{14}N NMR (21.7 MHz)

DMSO-d_6

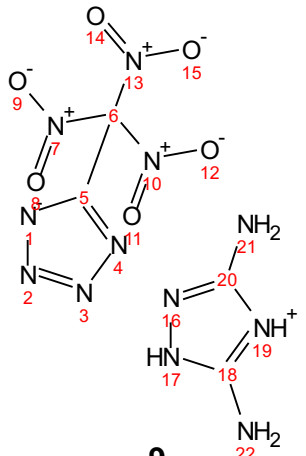

9

^{1}H NMR (300 MHz)

DMSO-d_6

7.05

DMSO

5.00

15.0 14.5 14.0 13.5 13.0 12.5 12.0 11.5 11.0 10.5 10.0 9.5 9.0 8.5 8.0 7.5 7.0 6.5 6.0 5.5 5.0 4.5 4.0 3.5 3.0 2.5 2.0 1.5 1.0 0.5 0.0

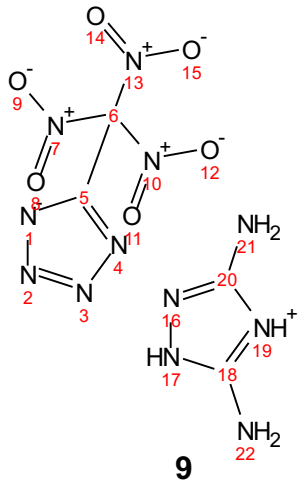

9

^{13}C NMR (75.5 MHz)

D_2O

150.32
149.37
123.63

210 200 190 180 170 160 150 140 130 120 110 100 90 80 70 60 50 40 30 20 10 0

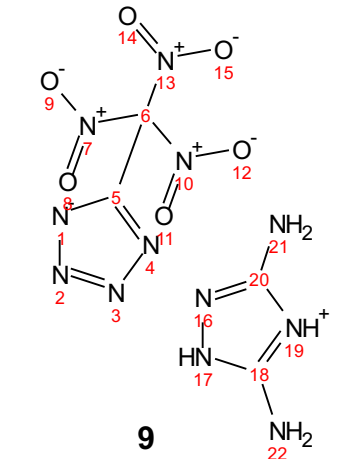

9

^{14}N NMR (21.7 MHz)

D_2O